

Applying the macroscopic chemistry method to dissociating oxygen

Charles R. Lilley* and Michael N. Macrossan†

**Department of Mathematics and Statistics, University of Melbourne, Melbourne, 3010, Australia*

†Centre for Hypersonics, School of Engineering, University of Queensland, Brisbane, 4072, Australia

Abstract. The macroscopic chemistry method was developed to model non-equilibrium chemically reacting flows with the direct simulation Monte Carlo (DSMC) method. The macroscopic method can use kinetic temperatures, calculated from mean particle energies, to calculate reaction rates. For strongly non-equilibrium flows, it is possible that using these mean energies could cause the macroscopic method to ignore reactions that should result from high-energy collisions that occur in the high-energy tail of the collision energy distribution. This could result in a “rate-reducing” effect relative to conventional collision-based DSMC chemistry models that perform reactions based on the energy of each individual collision. This effect would be most pronounced for reactions with low reaction energy. We test for this possible rate-reducing effect in the macroscopic method by calculating the hypersonic flow of dissociating oxygen, which has a low dissociation energy, over a blunt cylinder. The results are compared to those obtained with the most common collision-based DSMC chemistry model, the total collision energy model. The results are in close agreement and we observe no rate-reducing effect with the macroscopic method. This result extends the scope of the macroscopic method, and demonstrates its potential for modeling reacting non-equilibrium gas flows with the DSMC method.

Keywords: Direct simulation Monte Carlo, non-equilibrium chemistry

PACS: 47.11.-j, 47.70.Fw, 47.45.-n, 47.40.Ki

INTRODUCTION

The macroscopic chemistry method of Lilley & Macrossan [1] was developed to model flowfield chemistry in non-equilibrium flows with the direct simulation Monte Carlo (DSMC) method [2]. The macroscopic method adopts a decoupled approach to chemistry modeling, in which chemical reactions are decoupled from the DSMC collision routine. The chemical reactions are performed after the collision routine in an independent step. The macroscopic method uses macroscopic rate equations, with local macroscopic conditions derived from the DSMC simulation, to calculate the required number of reactions in each DSMC cell. This number of reactions is then performed, with reacting particles selected according to simple rules. To account for the chemical energy of the reactions, the thermal velocities of all particles in the cell are adjusted. The macroscopic method has been developed for the symmetrical diatomic dissociating gas, and has been successfully extended to capture the effects of vibration-dissociation coupling [3]. Lilley [4] gives full details of the macroscopic method.

The decoupled approach used in the macroscopic method represents a major departure from the conventional collision-based approach to modeling chemistry with the DSMC method. In collision-based DSMC chemistry models, chemical reactions are performed at the time of collision. When collision partners are selected, a reaction probability P_R is calculated. P_R is some function of the energies of the colliding particles. The form of P_R is chosen to plausibly approximate the expected real gas behaviour, subject to constraints imposed by mathematical tractability, numerical stability and computational efficiency, and to recover a suitable rate equation in the equilibrium limit. A reaction is performed if $R_f < P_R$, where R_f is a random fraction distributed uniformly in the range $[0,1]$. For dissociating nitrogen, the macroscopic method gives results that are generally in close agreement with conventional DSMC chemistry models and available experimental data [1, 3, 4].

The macroscopic chemistry method offers several significant advantages over conventional collision-based chemistry models.

- The macroscopic method can utilize *any* macroscopic rate expression, which may be *any* function of the macroscopic flow conditions. For example, Lilley & Macrossan [1] used the macroscopic method with a complicated form of the equilibrium constant that depended on number density as well as temperature. This equilibrium constant effectively controlled the recombination rate, and was applied to simulate the chemical relaxation of pure atomic nitrogen. The resulting relaxation behaviour was in excellent agreement with the exact solution. No mod-

els currently exist for capturing such relaxation behaviour with conventional collision-based DSMC chemistry models. The macroscopic method thus avoids the need to develop new collision-based DSMC chemistry models to recover the desired macroscopic rate behaviour. This versatility means that the large amount of literature on reaction rates can now be applied directly in DSMC calculations.

- Many conventional DSMC chemistry models have been developed for the variable hard sphere (VHS) collision model [5]. These chemistry models could be applied to other DSMC collision models, but the resulting reaction rates will differ from the expected rates due to different collision rates relative to the VHS model. The macroscopic method is simple to apply to *any* DSMC collision model, including realistic intermolecular potentials such as the Lennard-Jones potential, or realistic phenomenological DSMC collision models such as the generalized hard sphere model [6].
- As noted by Bird [2] and Lilley [4], conventional chemistry models can give a reaction probability P_R greater than unity, which is unrealistic. This results in a reduced net reaction rate realized by the DSMC solution as compared to the expected rate. The macroscopic method does not suffer from such numerical problems.
- The macroscopic chemistry method considers net reactions only. At equilibrium, there is no net change in composition and so no reactions are performed. Therefore the macroscopic method implicitly satisfies the detailed balancing requirement. Conventional DSMC chemistry models must consider the issue of detailed balancing at chemical equilibrium. This becomes difficult for reacting mixtures with many reactions between many species, and is further complicated by internal energy modes. Conventional DSMC chemistry models do not, in general, satisfy the detailed balancing requirement, and need further development to accomplish this [4].
- A further advantage of the macroscopic method is apparent in hybrid codes that use continuum solvers in near-equilibrium regions and the DSMC method in non-equilibrium regions. The macroscopic method allows the same chemistry model to be used throughout the entire simulation domain in such hybrid codes [4].

Given these advantages, combined with its versatility and apparent accuracy, it is clear that the macroscopic method offers significant potential for modeling non-equilibrium reacting gas flows with the DSMC method.

To date, the macroscopic method has only been applied to dissociating nitrogen, which has a relatively high dissociation energy. Here, we test the macroscopic method using dissociating oxygen. Our motivation for this is as follows:

The dissociation rate for the macroscopic method depends on local kinetic temperatures, or mean particle energies. In conventional collision-based DSMC chemistry models, the dissociation rate depends on the detailed distribution of energies in collisions. These distributions may be strongly non-equilibrium, and it is possible that collisions in the high-energy “tail” of the collision energy distribution could make a significant contribution to the net dissociation rate for the conventional models. Because the macroscopic method considers mean energies, it could conceivably miss such reactions and thus exhibit a reduced reaction rate. This “rate-reducing” effect would be most significant for molecules that have a low dissociation energy. Here we investigate the possible existence of the rate-reducing effect using oxygen, which has a low dissociation energy, by comparing hypersonic flowfield solutions obtained with the macroscopic method and the conventional total collision energy (TCE) chemistry model [7]. The hypersonic flowfield produces the strongly non-equilibrium conditions necessary for this test.

DSMC DETAILS AND RESULTS

For our test case, we considered the hypersonic flow of dissociating oxygen over an axisymmetric blunt cylinder. The flow geometry, freestream conditions and computational grid details are shown in Fig. 1. We used the VHS model which has the collision cross-section $\sigma(g) = \sigma_r (g_r/g)^{2v}$, where g is the relative speed in the collision and σ_r , g_r and v are the VHS parameters that are constants for each collision type. The reference relative speed g_r is arbitrary; we used $g_r = (2kT_r/\tilde{m})^{1/2}$, where \tilde{m} is the reduced mass of the collision pair and T_r is a reference temperature. For VHS molecules, it can be shown [4] that the mean collision cross-section $\bar{\Omega}$ is given by

$$\bar{\Omega}(T) = \sigma_r \frac{\Gamma(4-v)}{6} \left(\frac{T_r}{T} \right)^v.$$

Gupta *et al.* [8] provide $\bar{\Omega}$ expressions for O_2+O_2 , O_2+O and $O+O$ collisions that are valid to 30000 K. We used non-linear regression with $T_r = 1000$ K to find σ_r and v values that fitted the data of Gupta *et al.* The resulting VHS parameters are shown in Table 1.

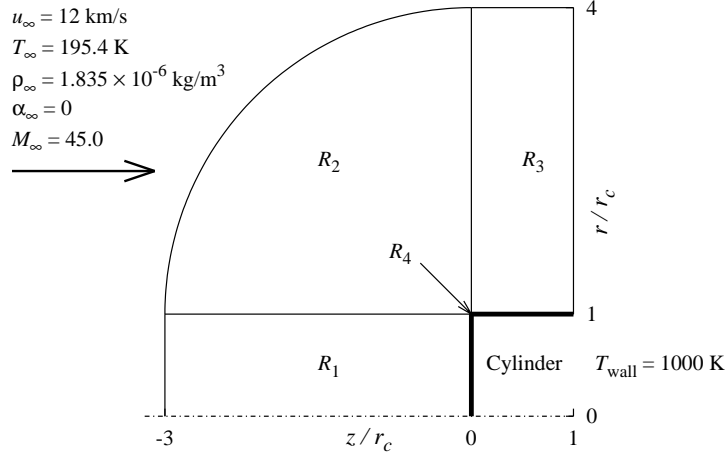


FIGURE 1. Blunt cylinder simulation geometry and freestream conditions. Flow is from left to right. Cylinder radius $r_c = 0.5$ metres. The simulation domain contained rectangular regions R_1 and R_3 and radial regions R_2 and R_4 . R_1 contained (180×200) cells in the $(z \times r)$ directions with a geometric progression in cell sizes in the z direction, increasing away from the cylinder. The ratio of Δz dimensions for adjacent cells, denoted f_z , was 1.0152. R_2 contained (180×90) cells in the $(d \times \phi)$ directions where d is the distance from the cylinder edge at $(0, r_c)$ and ϕ is the angle measured from the z -axis. For adjacent cells in R_2 , $f_d = 1.01$ with cell size increasing away from the cylinder, and $f_\phi = 1$. R_3 contained (70×120) cells in the $(z \times r)$ directions. In R_3 , $f_z = f_r = 1.01$ with cell size increasing away from the cylinder face. The small radial region R_4 contained only one cell, and extended to a distance $r_c/100$ from $(0, r_c)$. The cylinder wall was at 1000 K and fully diffuse reflection was used.

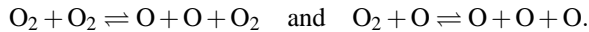
TABLE 1. Viscosity and VHS parameters for the dissociating oxygen system. $T_r = 1000$ K was used in all cases.

Collision partners	ν	σ_r (m ²)	g_r (m/s)
$O_2 + O_2$	0.158	3.939×10^{-19}	1019.5
$O_2 + O$	0.230	3.709×10^{-19}	1248.6
$O + O$	0.263	3.180×10^{-19}	1441.7

Using the VHS mean free path λ_{VHS} [2], the Knudsen number $Kn = \lambda_{VHS}/(2r_c) = 0.043$. This Knudsen number shows that rarefaction effects are important for this flowfield. A continuum breakdown parameter B , defined by $B = KnM_\infty$, is useful for characterizing hypersonic rarefied flows. For this case $B = 1.9$. These values of Kn and B both indicate that strongly non-equilibrium conditions are likely to prevail in the flowfield.

We used Borgnakke-Larsen procedures [9] to model internal energy exchange in the DSMC calculations, with the particle-based selection scheme of Gimelshein *et al.* [10]. This selection scheme permits different relaxation rates for different internal energy modes in each species. We used constant energy exchange probabilities of 0.3 and 0.01 for rotation and vibration respectively. Continuous rotational energy and quantized vibrational energy were used, for which exchange procedures are given by Borgnakke & Larsen [9] and Bergemann & Boyd [11]. The vibration model used unbounded harmonic oscillators with a characteristic temperature of 2270 K [12]. The simulation time step Δt was 3.20×10^{-7} s, and the sampling interval was $7\Delta t$. Cell-based weighting factors were used, and the mean number of particles per cell was ~ 20 at steady state. 1000 flowfield samples were collected.

Dissociation of pure diatomic oxygen proceeds via the two reactions



We used the Arrhenius dissociation rates provided by Gupta *et al.* [8], who give

$$k^+(T) = 6.07 \times 10^{10} (T/\Theta_d)^{-1} \exp(-\Theta_d/T) \quad \text{m}^3/\text{kmol/s}$$

for both reactions. This dissociation rate was used directly in the macroscopic method, and was used to calculate P_R for the TCE model following the method of Lilley [4]. For oxygen the characteristic dissociation temperature $\Theta_d = 59500$ K [12]. We ignored recombination reactions in this study.

The blunt cylinder flow was calculated with the TCE model and the macroscopic method. The stagnation streamline profiles of density, kinetic temperatures and dissociation fraction are compared in Fig. 2. The strongly non-equilibrium nature of the flow is clear from the different kinetic temperatures shown in Fig. 2: The translational kinetic temperature T_{tr} is higher than the rotational kinetic temperature T_{rot} which is higher than the vibrational kinetic temperature T_{vib} . Furthermore, the translational kinetic temperature in the z direction is much higher than that in the r and θ directions. (The θ direction is normal to the zr plane). Despite the strongly non-equilibrium conditions, close agreement in the profiles is evident for all aspects of the flow except T_{vib} , which agrees within about 30%. Fig. 3 compares the velocity and internal energy distributions sampled from a cell near $(z/r_c, r/r_c) = (-0.5, 0)$. Again, there is close agreement between the macroscopic and TCE solutions, despite the fact that these are strongly non-equilibrium distributions. As shown in Table 2, there is also close agreement between the coefficients of drag and heat transfer on the cylinder face. The macroscopic method and the TCE model have similar CPU requirements for this flow.

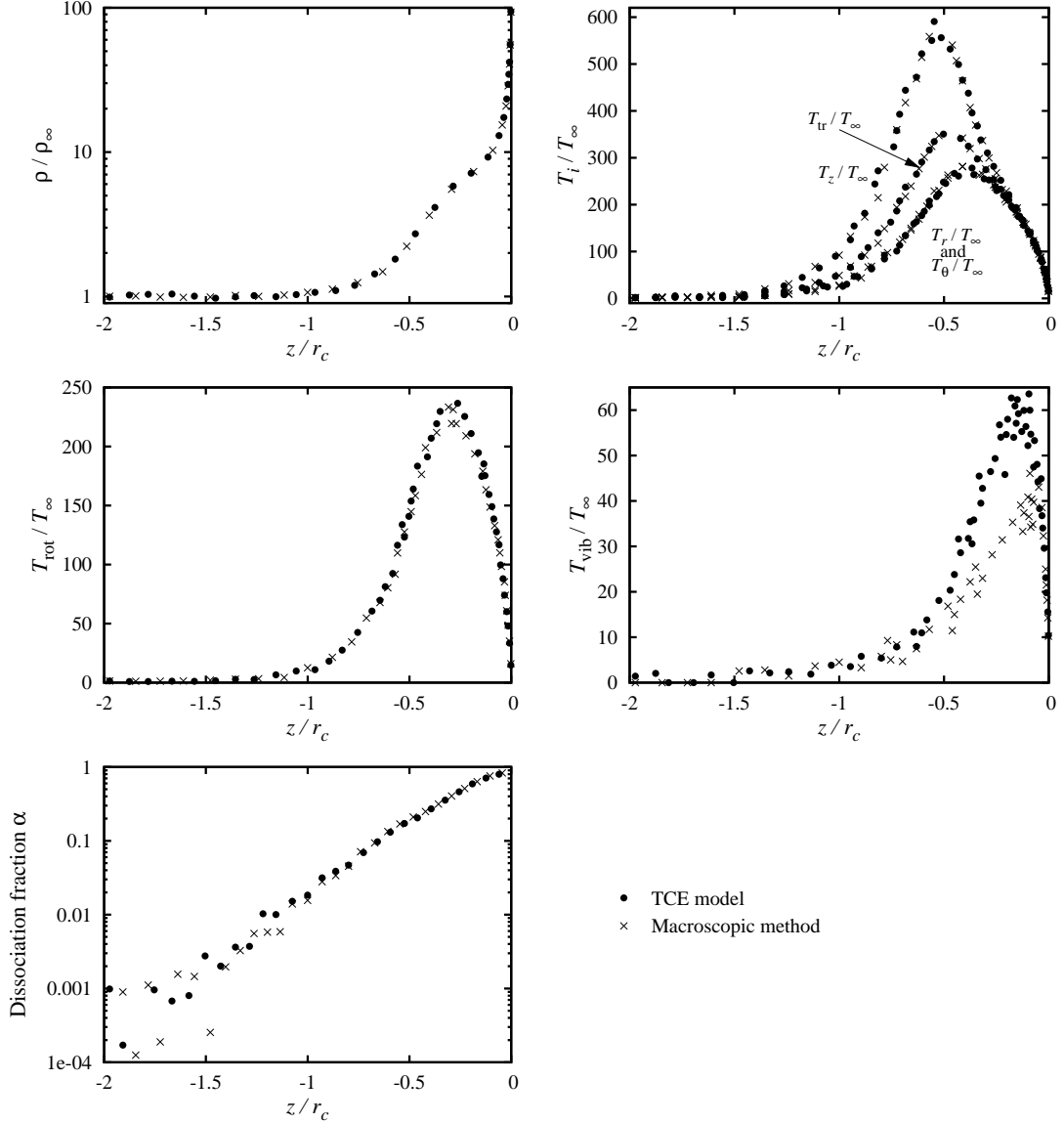


FIGURE 2. Profiles of normalized density ρ/ρ_∞ , translational kinetic temperatures T_z/T_∞ , T_r/T_∞ , T_θ/T_∞ and $T_{tr}/T_\infty = (T_z + T_r + T_\theta)/(3T_\infty)$, rotational kinetic temperature T_{rot}/T_∞ , vibrational kinetic temperature T_{vib}/T_∞ and dissociation fraction α along the stagnation streamline of the blunt cylinder in dissociating oxygen. Flow is from left to right. Flow geometry and freestream conditions are given in Fig. 1.

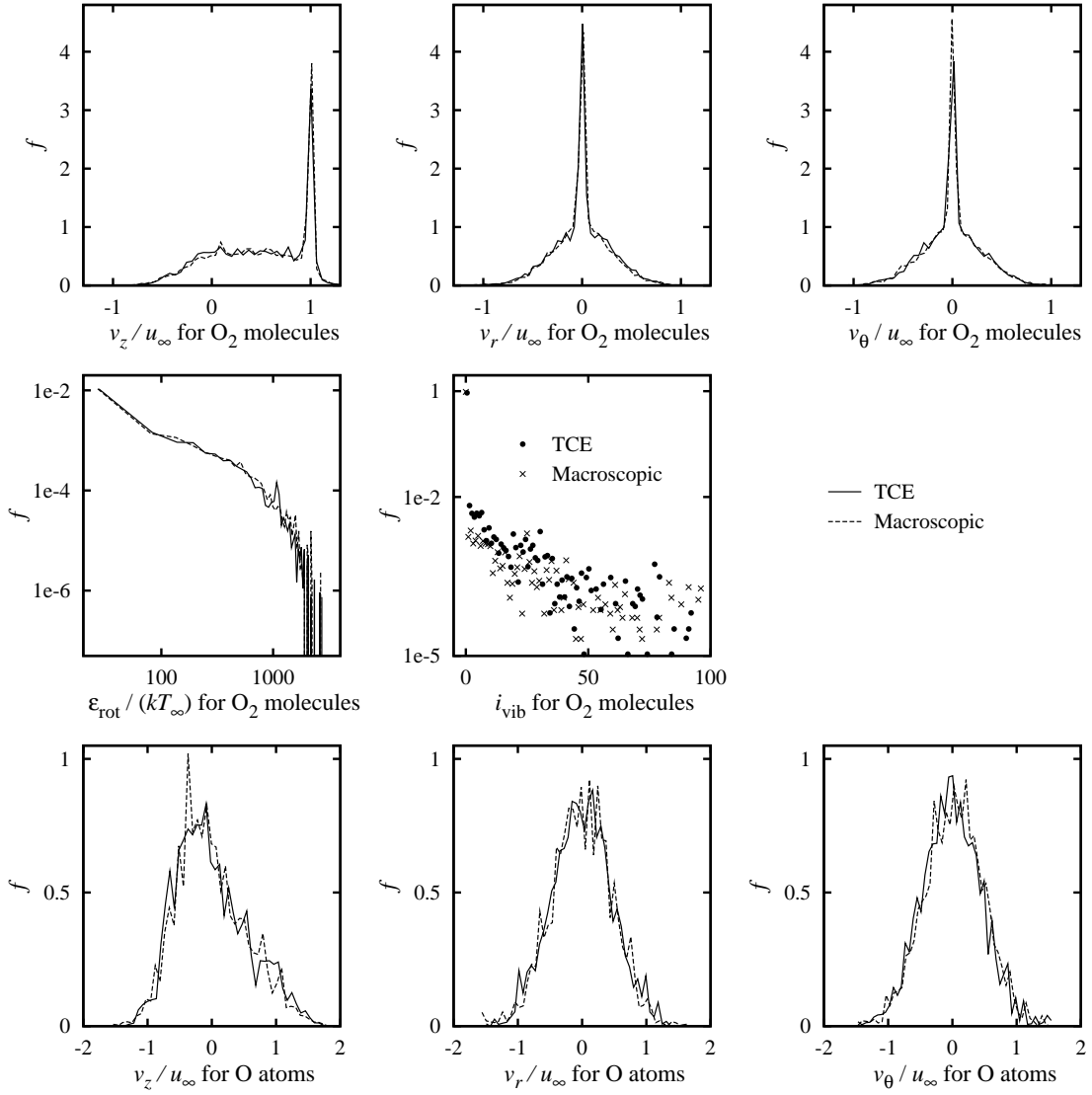


FIGURE 3. Distributions f of molecular velocities and internal energies sampled from a cell near $(z/r_c, r/r_c) = (-0.5, 0)$. Here v_z , v_r and v_θ are the molecular velocities in the z , r and θ directions respectively, ϵ_{rot} is the rotational energy and i_{vib} is the vibrational energy level. From Fig. 1, $u_\infty = 12$ km/s and $T_\infty = 195.4$ K.

TABLE 2. Comparison of drag coefficients C_D , heat transfer coefficients C_H , maximum dissociation fraction α_{max} and CPU requirements.

Solution	C_D	C_H	α_{max}	Relative CPU time
TCE model	1.755	0.258	0.815	1
Macroscopic method	1.755	0.261	0.836	0.97

DISCUSSION AND CONCLUSIONS

The agreement between the TCE and macroscopic solutions obtained here and previously [1, 3, 4] is not surprising. This is because chemical reactions are *infrequent events*, so the details of the chemistry model are relatively unimportant. For example, for the TCE results reported here, only 1.4% of $\text{O}_2 + \text{O}_2$ collisions and only 3.4% of $\text{O}_2 + \text{O}$ collisions resulted in a dissociation reaction. Provided we use the *correct reaction rate*, we can select reacting particles and

perform post-reaction energy disposal in any simple and convenient manner that is consistent with mass and energy conservation, with little effect on the overall flowfield. This was the original motivation for developing the macroscopic method, based on the work of Bartel *et al.* [13, 14]. The validity of this approach is demonstrated by the quality of the results.

The blunt cylinder flow case examined here used macroscopic reaction rate information in the common Arrhenius form. The macroscopic method applied this information directly, while the TCE model used it to calculate reaction probability P_R for each collision. The TCE model therefore applied the macroscopic Arrhenius rate information at the molecular level. Use of the TCE model implicitly assumes knowledge of the detailed reaction processes occurring at the molecular level, which are generally poorly known. The macroscopic method uses this same Arrhenius rate information and also applies it to non-equilibrium flows, but does not rely on detailed knowledge of reaction processes at the molecular level. In this respect, it the macroscopic method makes fewer assumptions than the TCE model, and thus constitutes a “safer” approach to modeling chemistry with the DSMC method.

The results presented here clearly show that there is close agreement between the TCE and macroscopic solutions for most aspects of the blunt cylinder flowfield. These results demonstrate that the macroscopic method is not subject to the possible rate-reducing effect induced by a strongly non-equilibrium distribution of collision energies. We expect that the macroscopic method can be extended to more complex reacting systems, as proposed by Lilley & Macrossan [1, 4], with acceptable accuracy relative to the TCE model.

ACKNOWLEDGMENTS

We acknowledge the valuable questions, comments and suggestions of Dr. Ingrid Wysong that prompted us to undertake this study. CL acknowledges support from the Department of Mathematics and Statistics at the University of Melbourne and the Particulate Fluids Processing Centre, a special research center of the Australian Research Council.

REFERENCES

1. C. R. Lilley, and M. N. Macrossan, *Phys. Fluids* **16**, 2054–2066 (2004).
2. G. A. Bird, *Molecular gas dynamics and the direct simulation of gas flows*, Clarendon Press, Oxford, 1994.
3. C. R. Lilley, and M. N. Macrossan, “Modeling dissociation-vibration coupling with the macroscopic chemistry method,” in *Rarefied gas dynamics: Proceedings of the 24th International Symposium*, edited by M. Capitelli, American Institute of Physics, New York, 2005, pp. 1019–1024.
4. C. R. Lilley, *A macroscopic chemistry method for the direct simulation of non-equilibrium gas flows*, PhD thesis, School of Engineering, University of Queensland (2005).
5. G. A. Bird, “Monte-Carlo simulation in an engineering context,” in *Rarefied gas dynamics: Proceedings of the 12th International Symposium*, edited by S. S. Fisher, AIAA, New York, 1981, vol. 74 of *Progress in Astronautics and Aeronautics*, Part I, pp. 239–255.
6. H. A. Hassan, and D. B. Hash, *Phys. Fluids A* **5**, 738–744 (1993).
7. G. A. Bird, “Simulation of multi-dimensional and chemically reacting flows,” in *Rarefied gas dynamics: Proceedings of the 11th International Symposium*, edited by R. Campargue, Commissariat à l’Energie Atomique, Paris, 1979, vol. 1, pp. 365–388.
8. R. N. Gupta, J. M. Yos, R. A. Thompson, and K.-P. Lee, *A review of reaction rates and thermodynamic and transport properties for an 11-species air model for chemical and thermal nonequilibrium calculations to 30 000 K*, NASA, Washington, 1990, NASA reference publication 1232.
9. C. Borgnakke, and P. S. Larsen, *J. Comp. Phys.* **18**, 405–420 (1975).
10. N. E. Gimelshein, S. F. Gimelshein, and D. A. Levin, *Phys. Fluids* **14**, 4452–4455 (2002).
11. F. Bergemann, and I. D. Boyd, “New discrete vibrational energy model for the direct simulation Monte Carlo method,” in *Rarefied Gas Dynamics: Experimental techniques and physical systems. Proceedings of the 18th International Symposium*, edited by B. D. Shizgal, and D. P. Weaver, AIAA, Washington, 1994, vol. 158 of *Progress in Astronautics and Aeronautics*, pp. 174–183.
12. W. G. Vincenti, and C. H. Kruger, *Introduction to physical gas dynamics*, John Wiley & Sons, New York, 1965.
13. T. J. Bartel, J. E. Johannes, and T. R. Furlani, “Trace chemistry modelling with DSMC in chemically reacting plasmas,” in *AIAA Paper 98-2753*, AIAA, Washington, 1998.
14. T. J. Bartel, “Modelling neutral and plasma chemistry with DSMC,” in *Rarefied gas dynamics: Proceedings of the 23rd International Symposium*, edited by A. D. Ketsdever, and E. P. Muntz, American Institute of Physics, New York, 2003, pp. 849–856.